CORROSION BEHAVIOUR OF 304L NAG AND 310L NAG IN NITRIC ACID: INVESTIGATION OF CAUSES AND PREVENTIVE STEPS

Shagufta Khan[1], Muhammad Hussain[2]
[1] AMCO Integrity Pty Ltd, Australia
[2] University of Wollongong (UOW), Australia

SUMMARY: Austenitic stainless steels (SSs) have been used as structural materials for various components in the aqueous reprocessing plants. These alloys are widely used in nuclear spent fuel reprocessing and waste management plants and the process fluid is nitric acid at temperature up to boiling point. Incorporation of oxidizing ions in nitric acid stream make the environment highly corrosive to stainless steels. Several types of nitric acid grade (NAG) alloys having compositions similar to Types 304L, 310L, and several new proprietary alloys have been developed worldwide. NAG alloys show lower corrosion rates compared to conventional Type 304L in boiling HNO_3 (Huey). However, several reports of failure have been reported in components made of NAG grade austenitic SS also. In this study it has been shown that the potential attained in process solution determines the corrosion behaviour of SS. Potentials were applied to Types 304 L NAG, and 310L in boiling 6 M nitric acid for a period of 48 h and corrosion behaviour was observed. Influence of Cr^{6+} concentration present in nitric acid solution on end grain corrosion rate was also studied. Some important observations of this investigation were: (1) Rate of IGC increased exponentially with the increase in the applied potential. (2) No significant difference in corrosion rate of Type 304L NAG1 having step and dual microstructures was observed (3) Increase in Cr^{6+} concentration present in nitric acid solution increase end grain corrosion rate of Type 304L NAG2.

Keywords: Steel, intergranular corrosion, transpassive potential, heat treatment, Microstructure, Nitric acid.

1. INTRODUCTION

1.1 Austenitic stainless steels (SSs) with low carbon content such as AISI types 304L, 310L, 347, 321, several other proprietary alloy steels having modified chemical composition and microstructures have been used as structural materials for various components in the aqueous reprocessing plants [1-4] Several types of nitric acid grade (NAG) alloys having compositions similar to Types 304L, 310L, and several new proprietary alloys have been developed worldwide [5]. NAG alloys show lower corrosion rates compared to conventional Type 304L in boiling HNO3 (Huey) test [6-9].This is achieved by (i) controlled chemical composition, (ii) modified microstructures leading to elimination of weaker sites for passive film break down and dissolution, and (iii) enhanced strength against transpassive dissolution. Increasing chromium content increases the stability and strength of passive film. However, in practice chromium levels below 30 % are used. The reason for this is that increase in chromium contents beyond this level affects the stability of the austenite phase. Nickel is another element which improves the strength of passive films through stabilizing austenite. Nickel is kept within 15% as increases in nickel content increases the cost of the alloy. Molybdenum is completely removed from the alloy due to two important reasons namely, (i) increasing ferrite formation, and (ii) submicroscopic sigma precipitation during multipass welding of components thicker than 6 mm. Sigma phase can preferentially dissolves in hot oxidizing HNO3 leading to excessive corrosion rates. Manganese, silicon, copper and aluminium are normally present as impurities in the steel making. Mn content less than 1 % is recommended to avoid inclusions. These inclusions are harmful as they are preferentially attacked in HNO3 service. Copper and aluminium are also reduced to low levels as they enhance selective corrosion attack in HNO3 service. Silicon has dual role with

respect to corrosion of Type 304L in HNO3. Good corrosion resistance is observed when Si content is less than 0.2%, and also when Si content beyond 1.6 % [5]. However, between 0.4 and 1% Si content, excessive IGC has been observed [5]. Hence, two grades of NAG alloys have evolved, one with Si less than 0.2%, and the other with 4% Si. The impurity elements like S, P and B significantly affect the corrosion resistance of Type 304L in HNO3 [5]. Sulphur forms MnS inclusions which degrade the alloy with selective dissolution. It is major cause of end grain corrosion or tunnel corrosion in Type 304L tubular and bar product [10]. Phosphorous is controlled within 200 ppm in NAG grade alloys and both S and P together within 250 ppm to ensure good corrosion resistance. Boron forms dichromium boride (ΔCr2B) along grain boundaries during quenching after solution annealing. This results in decrease in corrosion resistance of the conventional Type 304L and hence for NAG alloys, boron is not exceeded 10 ppm. In a typical Type 304, the carbon content range is 0.06–0.08%. During heat treatment in temperature regime 723–1073 K, carbon enhances the formation of chromium rich M23C6 carbide at grain boundaries [11-12].This leads to selective depletion of Cr in a narrow region adjacent to the grain boundary. M23C6 carbides, thus promotes excessive corrosion along the grain boundaries. Now a days ultra low carbon alloys with carbon levels less than 0.015% are being developed for HNO3. In this paper we have discussed the role of composition and microstructure ("step" and "dual") on corrosion behaviour of NAG SS in near boiling 6 M HNO3. Potentials were applied to NAG SS specimens in boiling 6M HNO3 for a period of 48 h. The corrosion rates measured in such experiments were plotted as a function of applied potential. Threshold potential, above which IGC was observed, was established with the help of these plots. Below this potential, uniform and low rate of corrosion occurred. Corrosion behaviour of Type 304L NAG1 and Type 310L NAG (all heat treated at 675 °C for 1h) were investigated and compared by Practice A, A262, ASTM, DL- EPR, tafel polarization, potentiostatic experiments and morphological study. Type 304L NAG1 specimens were subjected to various heat treatment in order to produce change in microstructure. The effect of microstructure on corrosion behaviour of Type 304L NAG1 was investigated. How presence of oxidising ion in nitric acid influence end grain corrosion was also investigated on tubular Type 304L NAG2.

2. MATERIALS AND EXPERIMENTAL DETAILS

2.1 Materials

The materials used for this study were austenitic SS Types 304L NAG1, and 310L NAG and 304 L NAG2. All three materials were in solution annealed condition. Types 304L NAG1 was obtained in the form of 3 mm thick plates, Type 310L was in form of tube having an outer diameter of 25.0 mm and an inner diameter of 21.7 mm. Type 304L NAG2 was in tube form having outer diameter 2.5 cm, and inner diameter 1.6 cm. The chemical composition of the materials is reported in Table 1. Test specimens having the ratio of total cross-sectional area to the total surface area of 14% were cut from the as-received materials. A set of specimens were further subjected to a sensitization heat treatment at 675°C for 1 h followed by water-quenching to simulate the worst microstructure in the HAZ of the weldment [14]. A few samples of Type 304L NAG 1 were also heat-treated at 675°C for 171 h to produce a "ditch" microstructure.

Table 1 Chemical composition of austenitic SS alloys used in the present study (wt %)

Elements	Composition (wt %)		
	Type 310L NAG	Type 304L NAG1	Type 304L NAG 2
Fe	Balance	balance	Balance
Cr	24.3	18.7	18.0
Mn	1.63	1.58	1.17
Ni	20.17	10.19	10.87
C	0.011	0.014	0.012
S	0.0005	0.004	0.003
P	0.019	0.024	0.018
Si	0.09	0.31	0. 25

2.2 Microstructural Characterization and Degree of Sensitization

The specimens of appropriate dimensions were cut from the Type 310L NAG, Type 304L NAG1 and Type 304L NAG2. Cross sectional and longitudinal sections of as- received and heat treated specimens were mounted in cold setting resin. Such sections were ground with silicon carbide papers and final polishing was done with a diamond paste to obtain 1 µm finish. The specimens were degreased in soap solution, rinsed in water and then dried with acetone. Electrolytic etching of the specimens was carried out in 10 % oxalic acid solution at a current density of 1 A cm-2 for 90 s as per practice A, A 262, ASTM [13]. Double-loop electrochemical potentiokinetic reactivation (DL-EPR) test was done on the samples to assess the degree of sensitization (DOS) [15]. A deaerated solution of 0.5 M sulfuric acid (H2SO4) + 0.01 M potassium thiocynate (KSCN) was used as the test solution in DL-EPR test. The detail methodology for conducting these tests were reported earlier [15].

2.3 Potentiodynamic Polarization Experiment

All potentiodynamic polarization experiments were carried out using a three-electrode system. The experimental setup was the same as reported in an earlier study [16]. This setup ensured that the acid concentration remained the same throughout the test. The test solution was 6 M HNO3 at a temperature (95°C) close to boiling point. The specimens were polished on successively finer grits of emery papers to 600 grit. A 2 mm diameter hole was drilled on one side of the specimen and a SS wire was used to provide electrical contact. The connecting wire was covered by an insulated sheathing and the contact surfaces between the specimen and the wire were covered using a polytetrafluoroethylene (PTFE) tape. The polarization curves were generated using a portable field potentiostat. The scan rate was 0.1 mV s–1.

2.4 Application of Potential on Austenitic Stainless Steel in Near Boiling 6 M HNO3

The setup was the same as described in the “Potentiodynamic Polarization Experiments” section. Potentials were applied using a potentiostat to an NAG sample immersed in 6 M HNO3. The exposure time was kept 48 h for each sample. The values of the applied potential were determined from the result of polarization experiments. Potentials ranged from passive to transpassive potentials. After the 48h exposure, the weight loss of the specimen was measured and corrosion rate was calculated by using method described earlier [16]. This test was performed on Type 304L NAG1 and Type 310L NAG2.

2.5 Study of End Grain Corrosion by Weight Loss Techniques

Type 304 LNAG2 was used to study “End Grain Corrosion”. The specimen geometry and size were chosen such that the cross sectional area was 32 % of total surface area of the specimen. Specimens were polished on successively finer grits of silicon carbide papers to a finish with 600 grit, cleaned with soap solution and dried with acetone. These specimens were used for practice C, A262, ASTM , end grain corrosion test, and OCP (open circuit potential) measurment. The test set-up and specimen preparation for end grain corrosion test were similar as it is for Practice C, A262, ASTM. Modification was done in test solution and test periods. Following test solution and test periods were used.

9M HNO3 + 1 g L-1 Cr6+, four periods each of 24 h duration.
9M HNO3 + 1.25 g L-1 Cr6+, twenty periods each of 3 h duration.
9M HNO3 + 1.5 g L-1 Cr6+, twenty periods each of 3 h duration.

2.6. Morphological Study

The morphology of corrosion attack on specimens after they were subjected to potentiostatic test and end grain corrosion test were studied with the help of optical microscope and SEM. SEM analysis was done in secondary electron imaging (SEI) and backscattered electron imaging (BEI) modes. In SEM analysis electron beam energy was kept 20 kV.

3. RESULTS AND DISCUSSIONS

3.1 Degree of sensitization

The microstructures of Type 304LNAG1 after electroetching in as-received condition and after different heat treatments are shown in figure 1. It showed “step” microstructure in as-received condition (figure 1a), “dual” microstructure when heat treated at 675 °C for 1 h (figure 1b). A few specimens of Type 304L NAG1 were heat treated at 675 °C for a extended period. Microstructure of Type 304L NAG1 remained “dual” even after heat treatment at 675 °C for 171h (figure 1c). Microstructure of Type 310L NAG in as-received condition is shown in figure 2a and after heat-treatment at 675 °C for 1 h in figure 2b.

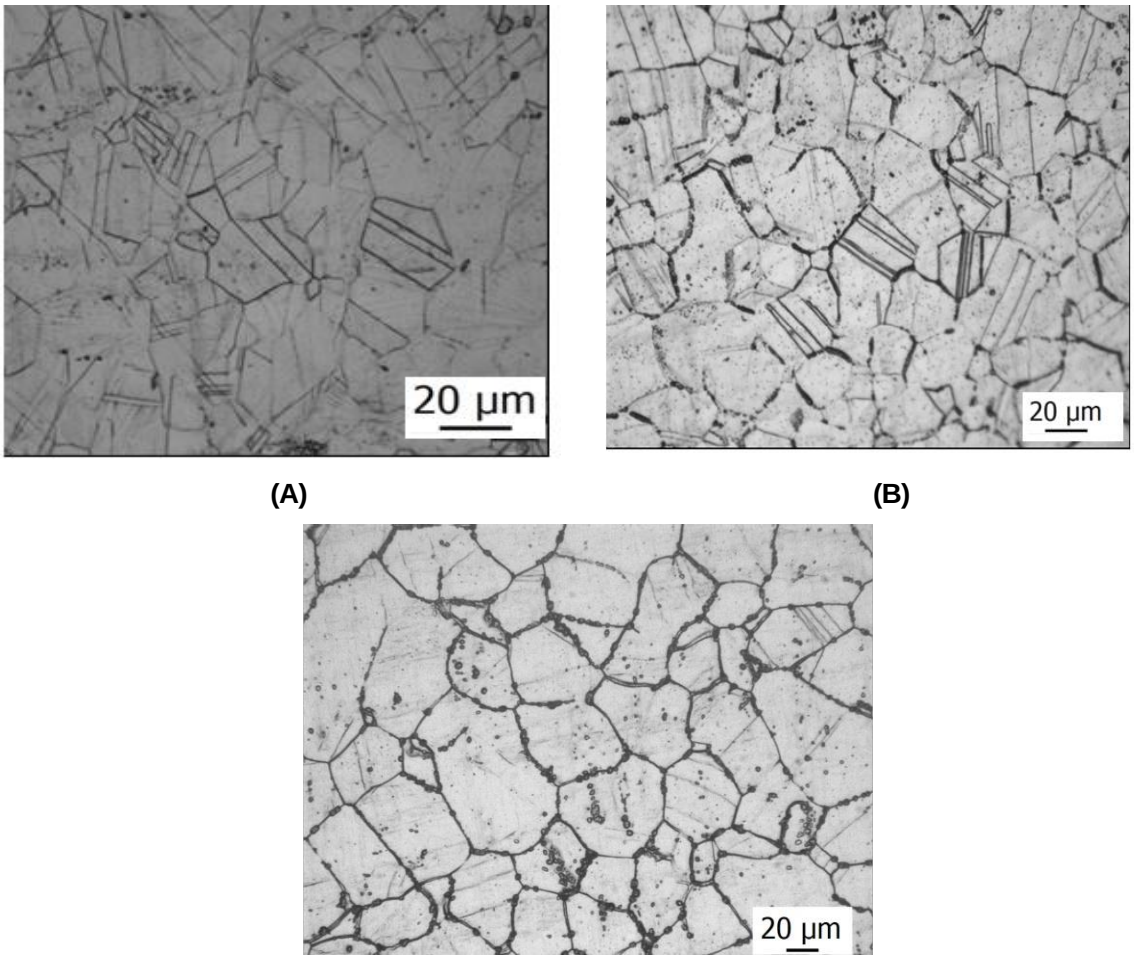

(A) **(B)**

(C)

Figure 1 Microstructural characterization of Type 304L NAG1 by optical microscope (a) as-received condition, (b) after heat treatment at 675 °C for 1 h and (c) after heat treatment at 675 °C for 171 h [17].

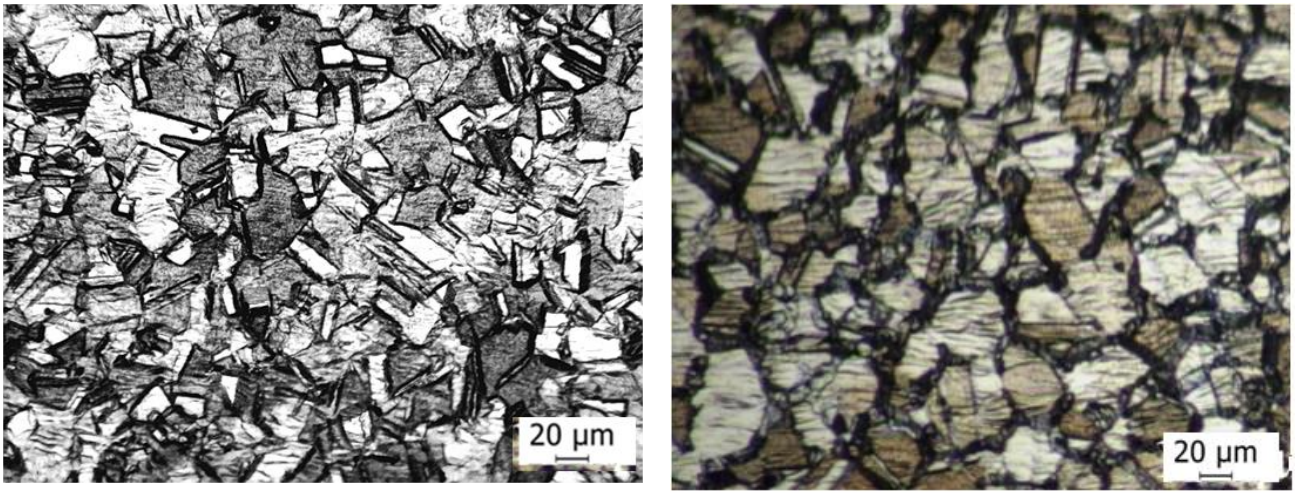

(a) **(b)**

Figure 2 Microstructural characterization of Type 310 L by optical microscope (a) as-received condition and (b) after heat treatment at 675 °C for 1 h [17].

DL-EPR tests have been performed to evaluate the degree of sensitization (DOS).It measures the extent of Cr depletion induced by $Cr_{23}C_6$ precipitation at grain boundaries or by any other phase formations, e.g., σ phase

[15]. Table 2 shows DOS for Type 304L NAG1 and Type 310L NAG in as- received condition as well as after different heat treatments. DOS values of Type 304L NAG1 specimens are (a) 0.14 for the as-received specimen (b) 0.50 for the specimen heat treated at 675 °C for 1h and (c) 0.17 for the specimen heat treated at 675 °C for 171h. These values indicated a very low value of DOS. Typically, a “ditch” microstructure is expected to have a DOS value of 5.0 or higher [18]. It has also been shown by systematic studies that it requires a DOS value above 5.0 to induce IGC in austenitic SS in practice C, A262, ASTM [18]. DOS for Type 310L NAG in the as-received condition and after heat treatment at 675 °C for 1 h were same. This implies that Type 310L did not get sensitized by the heat treatment given to it.

Table.2 Sensitization in Type 304L NAG1 and Type 310L NAG in as received and heat-treated condition

Material	Heat treatment	Degree of sensitization (DOS) (%)	Microstructure
Type 304L NAG1	As-received	0.11	Step
	675 °C for 1h	0.27	Dual
	675 °C for 171 h	0.17	Dual
Type 310L NAG	As-received	0.38	Step
	675 °C for 1h	0.38	Dual

3.2. Potentiodynamic polarization behavior

Figure 3 shows the potentiodynamic polarization curves for Type 304L NAG1 in near boiling 6M HNO3. The start of transpassive potential for these alloys was observed from Figure 3 to be 950–1000 mVSCE. Anodic current density was lower for Type 310L NAG than Type 304L NAG1 in the potential regime of 950–1000 mVSCE [17]. The Ecorr was established using Figure 3. The Icorr was established by extrapolating the linear part of the cathodic current and establishing its intersection with Ecorr. At Ecorr, the corrosion rate (Icorr) for Type 304L NAG1 and 310L NAG were found to be 9.7 x 10-6, and 5.7 x 10-6 Acm-2 respectively. The cathodic current density of Type 304L NAG1 was higher than for Type 310L NAG. The least rate of corrosion rate obtained in the case of Type 310L NAG could be explained from higher contents of Cr and Ni in Type 310L NAG compared to that in Type 304 L NAG1. Higher content of Cr is expected to lead to the formation of a passive film containing a higher amount of chromium and hence more protective. For “step” as well as “dual” microstructure of Type 304L NAG1 the value of OCP was very close to transpassive potential. Type 304L NAG1 having “dual” microstructure showed slightly lower value of transpassive potential compared to “step” microstructure.

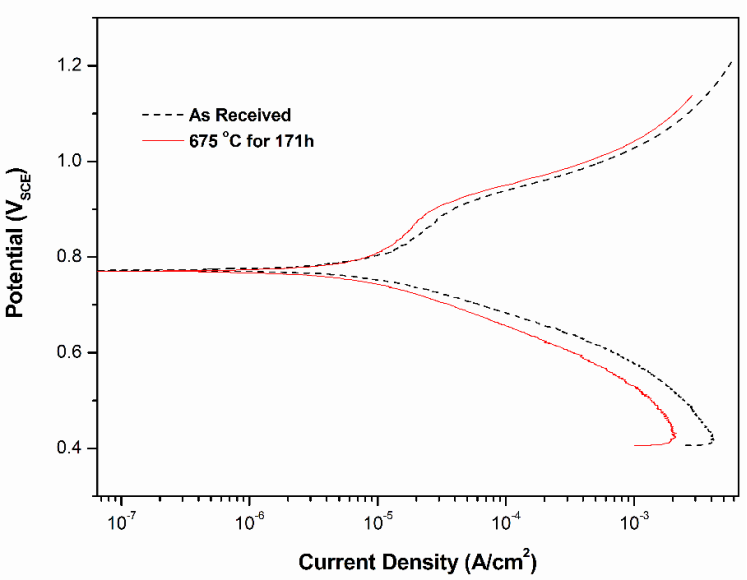

Figure 3 Polarization curves of Type 304L NAG1 in near boiling 6M HNO_3.

3.3 Potentiostatic tests conducted on Type 304L NAG1 and Type 310L NAG in 6M HNO3

Specimens of Type 304L NAG1 and Type 310L NAG heat treated at 675 °C for 1h were subjected to potentiostatic tests in near boiling 6M HNO3 as described in section 2.4. Corrosion rates (r) obtained in these tests were plotted

against applied potentials. Assuming an exponential dependence of corrosion rate on the applied potential, equation 1 was fitted to the data.

$$r = ae^{V/b} \quad \textbf{(1)}$$

where r is the corrosion rate (mmy-1) of SS upon exposure to near boiling 6M HNO3 for a period of 48 h, V is the applied potential (VSCE) and a and b are constants. Equation 1 can be rearranged to equation 2 which is a form of Tafel equation [1].

$$V = b \log \frac{r}{a} \quad \textbf{(2)}$$

The relationship between logarithm of corrosion rate (measured after 48 h exposures in near boiling 6M HNO3) and applied potential was confirmed to be a linear function, as shown in figure 4. The constants calculated using equation 2 for in Table 4.2.

Table.3 Constants calculated by fitting of equation 2 for Types 304L NAG2 and 310 NAG using figure 4

Type of SS	A (mmy^{-1})	B (V_{SCE})
310L	9.9×10^{-22}	0.0202
304L NAG1	9.8×10^{-26}	0.0180

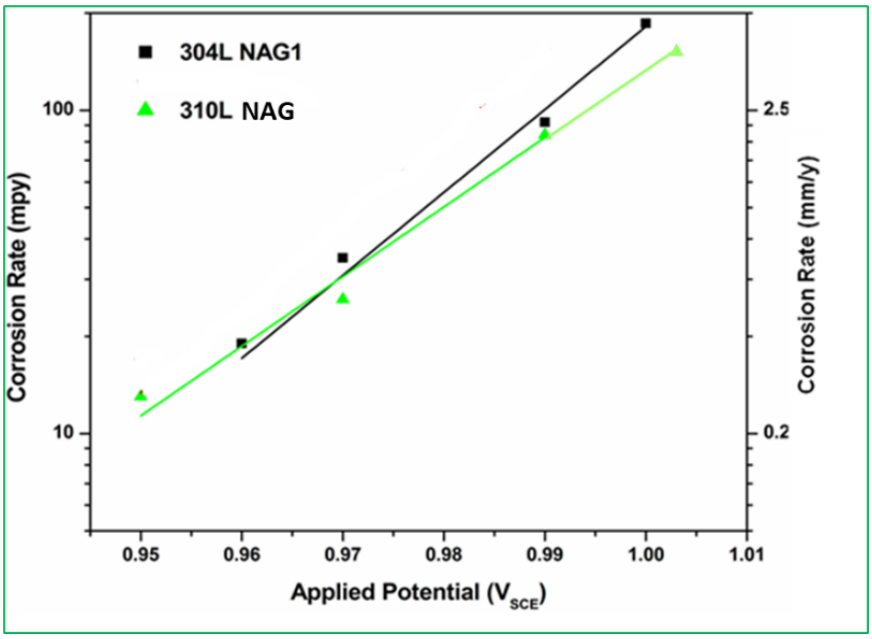

Figure.4 Correlation between corrosion rate (r) and applied potential (V) for Types 304 L NAG1 and Type 310L NAG heat-treated at 675 ℃ for 1 h exposed to near boiling 6M HNO_3 for 48 h.

These results indicated that potentiostatic application of potentials up to 0.95 V_{SCE} resulted in passivity being maintained on the SS specimens as only low rates of uniform corrosion could be observed on all the SS [17]. Potentiodynamic polarisation curves gave only a qualitative comparison of the corrosion tendency and could not

be used to predict the corrosion rate of SS at a given applied/developed potential. The corrosion rate at an applied potential for a given duration of testing has to be determined by the potentiostatic technique. These threshold potentials above which severe corrosion is observed would depend on type of SS and environment employed. It is evident from figure 4 that Type 310L NAG is more resistant to onset of IGC in the transpassive potential regime than Type 304L NAG1. This is in line with the observation of lower current density for Type 310L NAG in the potential regime of 950-1000 mV_{SCE} compared to that for Type 304LNAG1 [17]. Figure 5 and 6 show the morphology of corrosion attack on Types 304L NAG1 and Type 310LNAG sensitized at 675 °C for 1 h exposed to near boiling 6M HNO_3 for 48 h at a potential of 0.99 V_{SCE}. It is evident from figure 5 and 6 that the nature of corrosion attack is intergranular. The severity of corrosion attack is less in Type 310L NAG compared to Type 304L NAG.

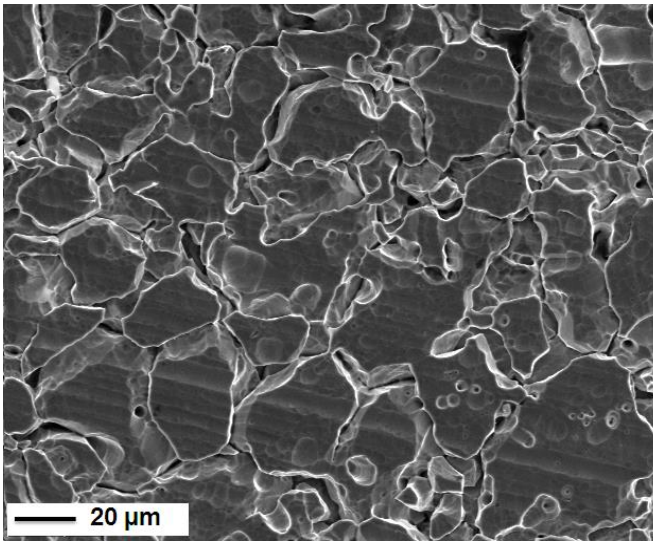

Figure 5. IGC observed after Type 304 L NAG1 heat-treated at 675 °C for 1 h and exposed to near boiling 6M HNO_3 for 48 h at 0.990 V_{SCE} under SEM [17].

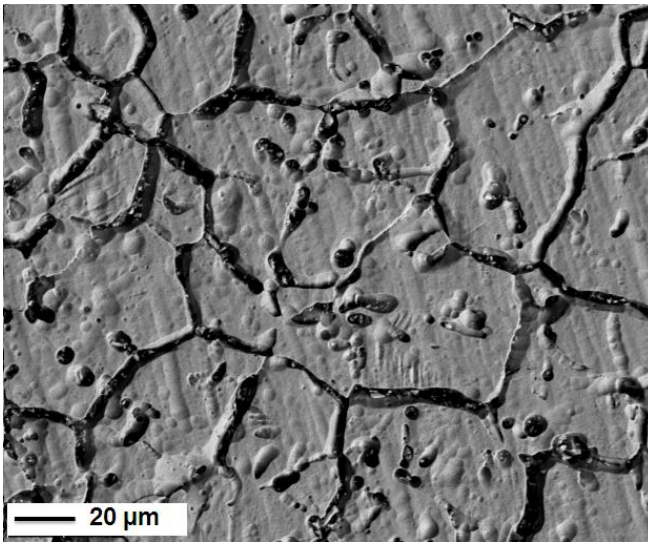

Figure 6. IGC observed after Type 310L heat-treated at 675 °C for 1 h and exposed to near boiling 6M HNO_3 for 48 h at (b) 0.990 V_{SCE} under SEM [17].

The relationship between logarithm of corrosion rate and applied potential for Type 304L NAG1 having “step” and “dual” microstructure is shown in figure 7 and constants calculated for the curve fitting using equation 2 corresponding to this figure are given in Table 4. From figure 7, it is indicated that the threshold potential for Type 304L NAG1 was (a) 0.967 for as received, (b) 0.966 V after heat treatment at 675 °C for 1 h and (c) 0.963 after heat treatment at 675 °C 171h. Corrosion rates for as-received and heat treated Type 304L NAG1 below the threshold potential (at 0.950-0.960 VSCE) are very low and are typical of corrosion rate of SS in the passivated condition below 0.51 mmy-1 (20 mpy). Type 304L NAG1 with “step” and “dual” microstructures showed comparable corrosion rates for entire range of applied potential. Various alloying elements are added to the steels to provide specific benefits in corrosion resistance, mechanical properties, or ease of fabrication. In the following paragraph the results obtained from the present investigation are correlated with compositional and microstructural factors. At a given applied potential, corrosion rates measured after 48 h immersion tests in near boiling 6M HNO3, were in the order of Type 310L < 304L NAG1. The carbon content of Type 304L NAG1 and Type 310L are 0.014 and 0.011 wt % respectively. It is clear that Type 310 L with least content of carbon is the more resistant to IGC than Type 304L NAG1. The role of carbon is easy to understand, since one of the major causes of susceptibility to IGC is the precipitation of chromium carbides [19, 20]. Carbon up to 0.07 percent by weight is soluble during annealing at 1066 °C. It has less than 0.01 percent solubility by weight at ambient temperature. Rapid cooling from the annealing temperature results in super saturation of carbon in solution. Subsequent holding in the sensitization range enables this carbon to precipitate out as chromium rich carbides. IGC susceptibility in austenitic SS increases as the carbon content increases [19, 20]. Chromium content in Type 310L and 304L NAG1 are 24.31and 18.72 wt.% respectively. The higher content of chromium in Type 310L can be associated with its lower corrosion rate at a given applied potential, in 48 h immersion tests in near boiling 6M HNO3. The addition of chromium increase corrosion resistance properties. Normally the amount of chromium in austenitic SS varies from 11 % to 25 % by weight. This amount is generally not sufficient to prevent attack in the oxidizing medium.

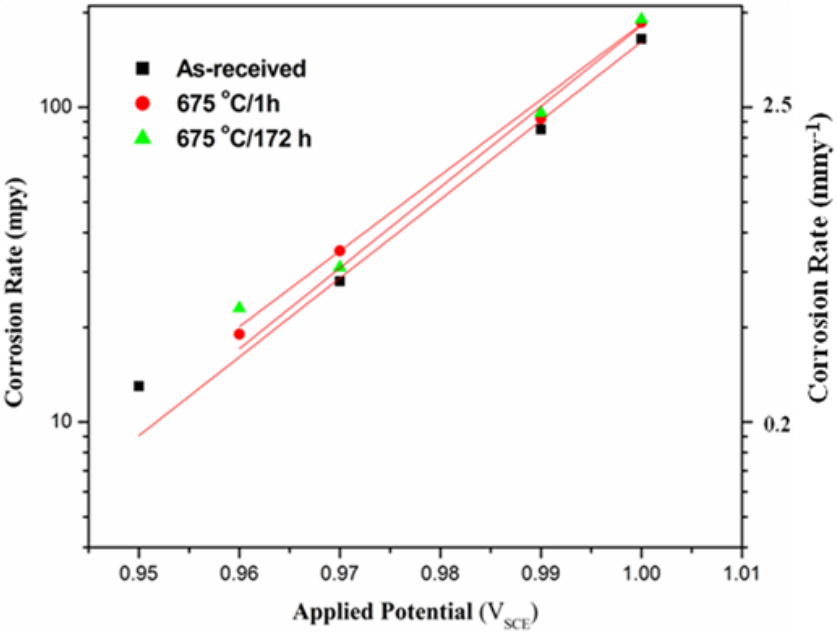

Figure. 7. Correlation between corrosion rate (r) and applied potential (V) for "step", and "dual" microstructures of Type 304L NAG1, exposed to near boiling 6M HNO_3 for 48 h.

Table 4 Constants calculated by fitting of equation 4.2 for Type 304L NAG1 having "step" and "dual" microstructure (Fig.7)

Microstructure	a (mmy^{-1})	b (V_{SCE})
Step	1.5×10^{-23}	0.01735
Dual	3.9×10^{-24}	0.01692
Ditch	1.6×10^{-22}	0.01807

The effect of Si content on IGC is more complex. Increase in IGC was observed up to 1 % Si content, after this limit IGC decreases when Si content increases IGC was not observed for Si values higher than 3 % in boiling HNO3 containing oxidizing species [1,2]. The silicon content of Type 304L NAG1 and Type 310L are 0.31 and 0.09 wt % respectively. It is clear that Si content is less than 1 wt % in both grades of alloys and it is the lower in Type 310L. Along with the higher content of Cr and the lower content of C, lower content of Si might be one of reasons for the least corrosion rate shown by Type 310 L at a given applied potential, in 48 h immersion tests in near boiling 6M HNO3. Increasing the bulk nickel content decreases the solubility and increases the diffusivity of carbon. This effect is much more pronounced when nickel content is above 20 %. It is generally recommended that in 25/20 Cr-Ni steel, carbon content should be less than 0.02 % to guarantee resistance to IGC. For the same reason the carbon content in Type 310L is 0.011 wt%.

3.4. End Grain Corrosion of Type 304L NAG2 at Different Concentrations of Cr6+

Type 304L NAG2 was in non-sensitized condition and showed "step" microstructure" (figure. 8) after electroetching in 10% oxalic acid. Specimen exposed to 9M HNO3 containing 1.5 g L-1 Cr6+ showed the highest corrosion rate while specimen exposed to 9M HNO3 containing 1g L-1 Cr6+ showed the least corrosion rate in end grain corrosion test. Trend of increase in corrosion rate with time was observed for all the three specimens. The corrosion rate for specimen exposed to 9M HNO3 containing 1.5 g L-1 Cr6+ in the 19th period was 23 mmy-1 (909 mpy). The corrosion rate of the specimen exposed to 9M HNO3 containing 1.25 g L-1 Cr6+ in 19th period was 17.4 mmy-1 (688 mpy). Specimen exposed to 9M HNO3 containing 1g L-1 Cr6+ in showed a corrosion rate of 8.4 mmy-1 (332 mpy) after the same exposure period (57 h). The corrosion attack as seen in the longitudinal direction of the specimen was typical end grain corrosion as seen in figure 10. The depth of end grain corrosion in the specimen exposed to boiling 9M HNO3 containing 1.5 g L-1 Cr6+ after 19th period was 475 µm. The depth of the end grain corrosion in specimen exposed to boiling 9M HNO3 containing 1.25 g L-1 Cr6+ after 20th period was 100 µm. The potential developed when specimens were exposed to boiling 9M HNO3 containing different concentrations of Cr6+ ions is increased with increase in Cr6+ concentration. The higher potential developed on

the specimen exposed to boiling 9M HNO3 containing 1.5 g L-1 Cr6+ may be the reason for higher corrosion rate and very deep end grain corrosion attack observed in this specimen.

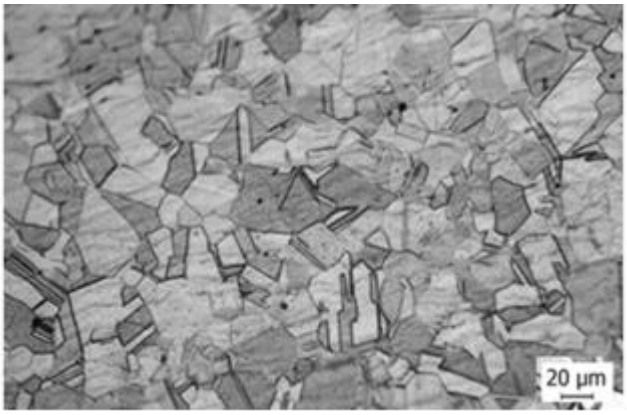

Figure 8 Microstructure of Type 304L NAG2 observed by optical microscope in as received condition.

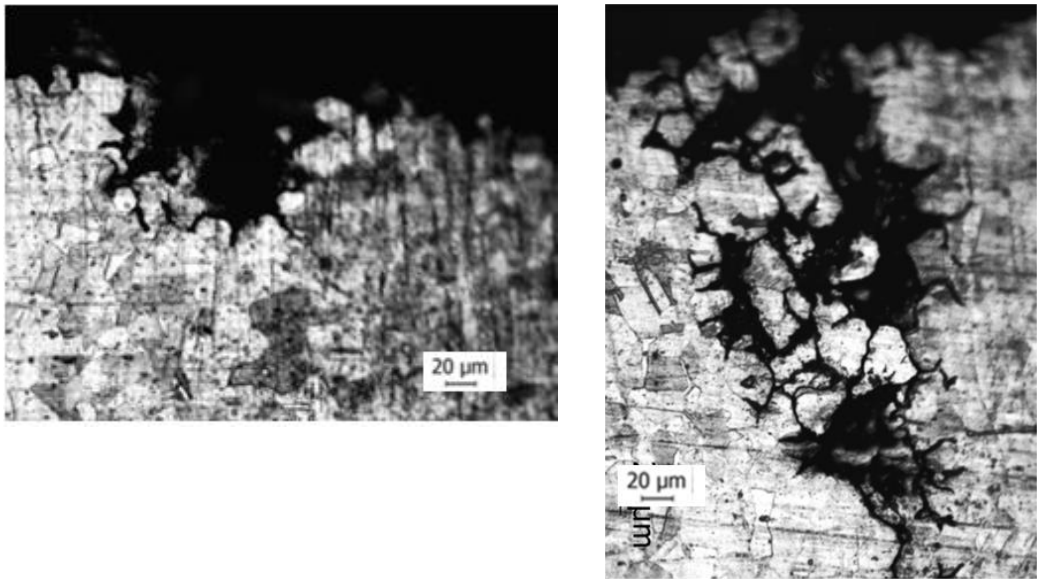

(a) **(b)**

Figure.10. Corrosion attack as seen in the longitudinal direction of specimen by optical microscope exposed to 9M HNO_3 containing (a) 1.25 g L^{-1} Cr^{6+} and (b) 1.5 g L^{-1} Cr^{6+}.

4. CONCLUSIONS

From present investigations following conclusions were drawn.

- Intergranular nature of corrosion of austenitic SS was clearly dictated by transpassive potential in HNO_3.
- Corrosion rate measured after 48 h immersion tests in near boiling 6M HNO_3 increased exponentially with the increase in the applied potential for Type 304 L NAG1 and Type 310L NAG.
- At a given applied potential, corrosion rates measured after 48 h immersion tests in near boiling 6M HNO_3, were in the order of Type 310L < 304L NAG1.
- "Ditch" microstructure could not be produced in Type 304L NAG1 by chosen heat treatment. There was no significant difference in corrosion rate of Type 304L NAG1 having step and dual microstructures.
- Increase in Cr^{6+} concentration in 9M HNO_3 increased Type 304L NAG2 susceptibility to end grain corrosion.
- This increase in susceptibility to end grain corrosion of Type 304L NAG2 is attributed to increase in electrochemical potential with increase in Cr^{6+} concentrations.

5. REFERENCES

1. Fauvet, P. (2012), “Corrosion issues in nuclear fuel reprocessing plants”, in Feron, D. (Ed.), Nuclear Corrosion Science and Engineering, Woodhead Publishing, Cambridge, pp. 679-728.
2. Fauvet, P., Balbaud, F., Robin, R., Tran, Q.T., Mugnier, A. and Espinoux, D. (2008), “Corrosion mechanisms of austenitic stainless steels in nitric media used in reprocessing plants”, Journal of Nuclear Material, Vol. 375, pp. 52-64.
3. Tcharkhtchi-Gillard, E., Benoit, M., Clavier, P., Gwinner, B., Miserque, F. and Vivier, V. (2016), “Kinetics of the oxidation of stainless steel in hot and concentrated nitric acid in the passive and transpassive domains”, Corrosion Science, Vol. 107, pp. 182-192.
4. Robin, R., Miserque, F. and Spagnol, V. (2008), “Corrosion mechanisms of austenitic stainless steels in nitric media used in reprocessing plants”, Journal of Nuclear Material, Vol. 375 No. 1, pp. 65-71.
5. A. J. Sedriks, Corrosion of stainless steels, second ed., John Wiley and Sons, New York, NY, 1996.
6. Baldev Raj, U. Kamachi Mudali, Prog. Nucl. Energ., 48 (2006) 283.
7. H.S. Ahluwalia, M. Davies,Te-Lin Yau, Corrosion by Nitric Acid, in: S. D. Cramer, B. S. Covino (Eds), Corrosion: Environments and Industries, Vol 13C, ASM Handbook, tenth edition, ASM International , Ohio, 2006, p 668-673.
8. V. Kain, S. S. Shinde and H. S. Gadiyar, Mechanism of improved corrosion resistance of type 304 L stainless steel, nitric acid grade, in nitric acid environments, J. Mater. Eng. Perf., 3 (1994) 699-705.
9. V. Kain, P. Sengupta, P. K. De and S. Banerjee, Case reviews on the effects of microstructures on the corrosion behavior of austenitic alloys for processing storage of nuclear waste, Metall. Mat. Trans. A, 36 A (2005) 1075-1084.
10. V. Kain, S.S. Chouthai, and H.S. Gadiyar, Performance of AISI 304L stainless steel with exposed end grain in intergranular corrosion tests, Brit. Corr. J., 27 (1992) 59-65.
11. J. S. Armijo, Intergranular corrosion of non sensitized austenitic stainless steels, Corrosion, 24 (1968) 24-30.
12. J.Y. Jeng et al, Laser surface treatments to improve the intergranular corrosion resistance of 18/13/Nb and 304 in nitric acid, Corr. Sci., 35 (1993) 1289-1296.
13. ASTM designation A-262, Practice B in annual book of ASTM standards, ASTM Philadelphia, PA, 2005
14. M. H. Brown, Corrosion, 30 (1974) 1.
15. V. Cíhal, T. Shoji, V. Kain, Y. Watanabe, R. Stefec, “EPR – AComprehensive Review,” FRRI Publication (Tohoku University, Japan: 2004).
16. S. Bhise, V. Kain, Corros. Eng. Sci. Techn. 47 (2011): p. 61-69.
17. Shagufta Khan Ph.D. thesis, Corrosion of austenitic stainless steels in nitric acid at transpassive potentials: Effect of materials and process parameters, 2016, HBNI, India.
18. A. P. Majidi, M. A. Streicher, Corrosion, 40 (1984) 584.
19. M. G. Fontana, Corrosion Engineering, third ed., Tata McGraw-Hill Publishing Company Limited, New York, 2005.
20. D.A. Jones, Principles and Prevention of Corrosion, second ed., MacMillan Publishing Co., 1992.

6. AUTHOR DETAILS

Dr Shagufta Khan has 13 years of experience in research and development and training.
She has published 15 research papers in international journals and conference proceedings. She has presented her research work in several international conferences.

Professional Expertise:

- Corrosion Management
- Quality management
- Metallurgy of ferrous metals and precious metals.
- Precious metals assay technology

Mr. Hussain has over 10 years' experience in improving business outcomes by driving up pipeline performance while reducing cost and risk through managing asset reliability.

Professional Expertise:

- Pipeline Integrity Management
- Corrosion Management
- Asset Management
- Fitness for Service (FFS)
- Big Data Analysis